

# Full-field heterodyne interference microscope with spatially incoherent illumination

Mark C. Pitter, Chung W. See, and Michael G. Somekh

*Applied Optics Group, School of Electrical and Electronic Engineering, University of Nottingham, Nottingham NG7 2RD, UK*

Received February 2, 2004

A heterodyne interference microscope arrangement for full-field imaging is described. The reference and object beams are formed with highly correlated, time-varying laser speckle patterns. The speckle illumination confers a confocal transfer function to the system, and by temporal averaging, the coherence noise that often degrades coherent full-field microscope images is suppressed. The microscope described is similar to a Linnik-type microscope and allows the use of high-numerical-aperture objective lenses, but the temporal coherence of the illumination permits the use of a low-power achromatic doublet in the reference arm. The use of a doublet simplifies alignment of the microscope and can reduce the cost. Preliminary results are presented that demonstrate full-field surface height precision of 1 nm rms. © 2004 Optical Society of America

OCIS codes: 180.3170, 120.5050, 180.1790.

It is possible to measure interference phase and amplitude in very small bandwidths (typically 1 kHz or less) if optical heterodyne techniques and phase-sensitive detection are applied to interference microscopy. Heterodyne interference microscopes have generally used focused coherent illumination and scanning, as this provides a confocal transfer function and reduces coherence noise. Full-field heterodyne imaging can be performed with coherent light,<sup>1,2</sup> but the confocal properties are lost. The use of spatially incoherent illumination in heterodyne interference microscopes could allow for full-field confocal imaging free from coherence noise.<sup>3</sup> Hitherto, scanning has generally been used in practice because of the difficulty of frequency shifting spatially incoherent light and the lack of detector arrays that can respond to intensity-modulated light. However, custom CCD and complementary metal-oxide semiconductor detector arrays<sup>4–6</sup> have begun to be used to address the latter problem and also hold out the possibility of building ultrastable microscopes by use of an optically generated local oscillator.<sup>2</sup> The difficulty of frequency shifting spatially incoherent light is bypassed in the illumination scheme described below.

The interference microscope described here uses diffuse (speckled) laser light such that the object and reference beams are temporally coherent but spatially incoherent. Confocal action arises in the microscope from the correlation between the reference speckle pattern and that reflected from the sample. That is, decorrelation of the object speckle pattern as it defocuses results in a reduction of the interference signal.<sup>3</sup> Coherence noise in the image is reduced by temporal averaging over many speckle patterns. Cross talk between adjacent pixels is determined entirely by confocal point-spread function, and pixels more than this distance away will not correlate with the reference and will therefore contribute a signal that averages to zero when the coherence noise is averaged.

These effects could be obtained by using a thermal source, but speckled laser light has far greater temporal coherence. This allows for flexibility in the design of microscope optics and is demonstrated here with an interference microscope with mismatched optics in the object and the reference arms.

A diagram of the microscope illumination is shown in Fig. 1. In an arrangement similar to a Mach–Zehnder interferometer, light from the laser passes through a half-wave plate and is split into vertical and horizontal components by a polarizing beam splitter, PB1. These two beams will eventually illuminate the object and reference arms of the interference microscope. The half-wave plate is used to control the input polarization and hence the object/reference beam power ratio. Each of the beams is passed through an acousto-optic modulator (AOM or Bragg cell). The +1-order output beams

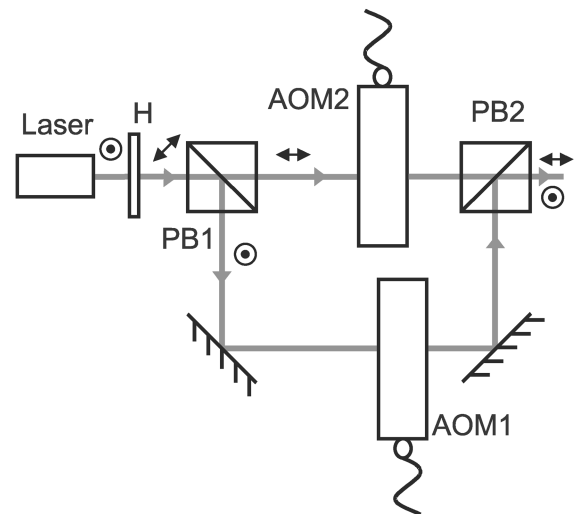


Fig. 1. An illumination-arm outputs two orthogonally polarized collinear beams, using a half-wave plate (H), polarizing beam splitters (PB1 and PB2), and acousto-optic modulators (AOM1 and AOM2).

from the AOMs are efficiently recombined at a second polarizing beam splitter, PB2, so that they are highly collinear and coaxial.<sup>2</sup>

The dual output beam has properties similar to those of a Zeeman laser. However, the arrangement described here allows far greater design flexibility. The output power and wavelength can be selected from a large choice of available laser source technologies, the optical frequency shift between the two beams is variable and can be dynamically controlled, and the relative path length of the two arms can be controlled. Two AOMs, driven by locked oscillators, are used so that relative frequency shifts from dc to tens of millihertz can be achieved. The ability to work at heterodyne beat frequencies of a few hertz is essential when one is imaging with readily available CCD cameras and cannot be achieved with a single AOM. The use of two AOMs also suppresses the effects of unwanted reflections from the Bragg cells<sup>7</sup> and electrical interference from the AOM drivers.

The imaging and reference optics are illustrated in Fig. 2. The dual illumination beams are incident upon the rotating diffuser, D, creating two orthogonally polarized and highly correlated incoherent sources. This arrangement allows frequency shifting to be applied to spatially coherent laser beams while retaining the advantages of spatially incoherent microscope illumination described above. Condenser lens C images the dual sources into the back focal planes of the low-power reference-arm lens L1 and a microscope objective, MO. Polarizing beam splitter PB ensures that the vertically polarized source is used to illuminate the object arm and the horizontally polarized source is used for the reference arm. The object beam passes through the microscope objective to the sample, where it is reflected and imaged by the microscope objective and tube lens L2 onto a detector array. The reference beam passes through L1 to a reference mirror, M, where it is imaged by L1 and L2 onto the detector array. The double passage through the quarter-wave plates in each arm rotate the polarization state of each beam through 90°. The sample and the reference mirror are therefore illuminated with circularly polarized light. A linear polarizer (P) with its axis between vertical or horizontal is placed in front of the detector array to allow the signal and reference beams to interfere. Adjusting the angle of P changes the relative amplitudes of the object and the reference beams and so controls the image interference contrast. The mismatch in optical path length caused by this arrangement is  $4(f_{L1} - f_{MO})$ , where  $f_{L1}$  and  $f_{MO}$  are the focal lengths of reference lens L1 and objective lens MO, respectively, and can be hundreds of millimeters. For optimal interference at the detector array this mismatch is canceled by unbalancing the illumination-arm path lengths, a correction that is easily achieved with this illumination arrangement.

The microscope optics described above are similar to the Linnik arrangement<sup>8</sup> in that the illumination is split and recombined behind the microscope objective lens rather than in front of the lens as in the Mirau and Michelson arrangements. This allows

the use of high-N.A. objective lenses with arbitrarily short working distances. Linnik microscopes use a matched pair of high-quality microscope objectives to ensure that the reference and object beams interfere efficiently. This is essential if sources with significant linewidth are used because the dispersion and the optical path length must be closely matched across the entire useful field in each arm. The need for dispersion matching is eliminated here, and the need for path-length matching is greatly reduced by use of diffuse but narrowband laser light. This allows the use of simpler low-power reference optics and reduces reference alignment tolerances. The results below were obtained with either a Zeiss 5× achromatic microscope objective (N.A. 0.13, focal length approximately 33 mm) or a Zeiss 50× (N.A. 0.7, focal length approximately 3 mm) in the object arm combined with an achromatic doublet in the reference arm (focal length 100 mm). This arrangement is particularly resource effective when a high-quality microscope objective is used, as only one is required, rather than a matched pair.

The microscope setup described above was used at low heterodyne frequency with a CCD camera to investigate the imaging properties. The heterodyne beat frequency was set to 1 Hz, and a CCD camera acquired a sequence of four images near 4 Hz. The Carre algorithm was used to estimate the phase at all points in the image.<sup>9</sup> Figure 3(a) is a phase map of an aluminum-coated etched glass grating (depth 17 nm, pitch 80 μm) as obtained with the microscope. Figure 3(b) shows a horizontal curve across the sample. The 17-nm steps are clearly resolved. A vertical section is shown in Fig. 3(c). The rms phase variation is approximately 1 nm. Figure 4 shows a similar result obtained from a resolution target by use of a 50×, 0.7-N.A. microscope objective lens. The chrome is approximately 50 nm thick.

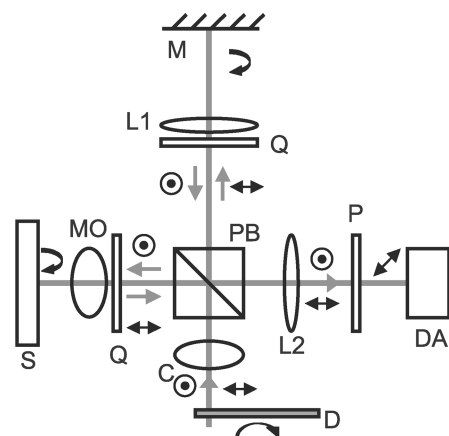


Fig. 2. Incoherent but highly correlated beams scattered by moving diffuser D are collected by condenser C and separated by polarizing beam splitter PB. Images of the diffuse source are formed in the back focal planes of the microscope objective (MO) and reference lens L1. Light from the object arm (MO, quarter-wave plate Q, and sample S) and the reference arm (L1, quarter-wave plate Q, and mirror M) is imaged onto detector array DA by tube lens L2. Polarizer P allows the beams to interfere.

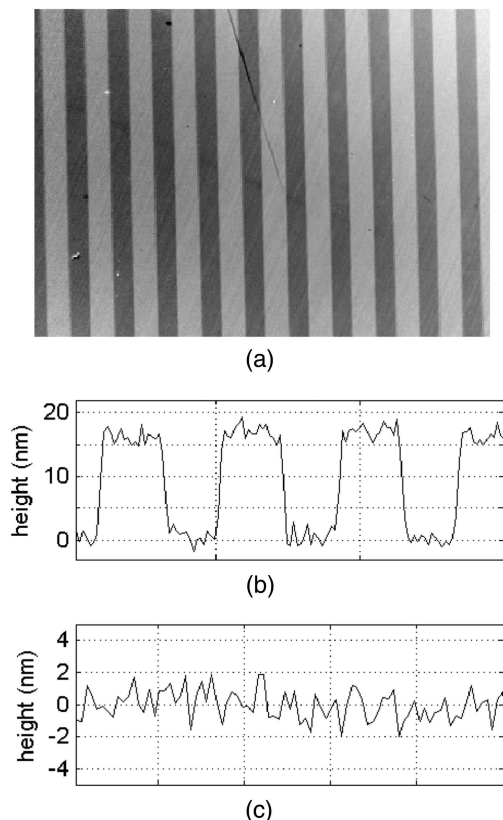


Fig. 3. (a) Phase map measured at a N.A. of 0.13 from an aluminum-coated glass grating of depth 17 nm and pitch  $80\ \mu\text{m}$ . (b) Horizontal and (c) vertical sections through (a).

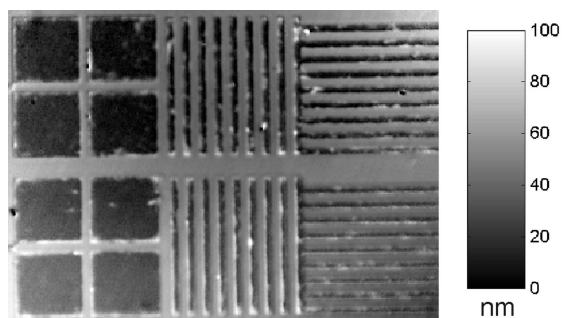


Fig. 4. Height map in nanometers measured at a N.A. of 0.7 from a chrome-on-glass resolution target. The vertical slots are  $1.375\ \mu\text{m}$  wide.

We have described and demonstrated a confocal heterodyne wide-field microscope in which confocality is established by interfering two similar but spatially incoherent beams. The large temporal coherence of the laser source confers an enormous advantage in that it enables the reference speckle pattern to be produced with two dissimilar lenses. The prototype setup used here demonstrates the use of low-power (0.13-N.A.) and higher-power (0.7-N.A.) microscope objective lenses, and the choice of lens is unrestricted by the need to insert beam-splitting optics between the lens and the sample.

Depth resolution in this system is provided by the spatial coherence of the illuminating beams and is therefore determined by the illuminating wavelength divided by the square of the numerical aperture of the objective lens. Efficient interference can occur only when the speckles are recombined exactly in three dimensions, and since the size of the speckles is diffraction limited, the imaging has enhanced lateral and depth resolution compared with coherent full-field imaging (identical to scanned confocal or scanned heterodyne imaging). This has been confirmed by measurement. The effect of the speckle on the performance of conventional heterodyne detection techniques is currently being investigated.

In optical coherence tomography depth resolution is provided by reduced temporal coherence (rather than spatial coherence). Both approaches may be used to achieve depth resolution, but in general the confocal approach will have better depth resolution when the N.A. is high.

The microscope presented here combines the advantages of heterodyne detection with the robustness of spatially incoherent illumination. We believe that this approach will have a major effect when pixellated ac detectors building on the work described in Refs. 4–6 become more widely available. These detectors will give improved dynamic range over CCD detectors, since the shot noise will no longer be limited by the well capacity of the CCD. The approach will also allow high heterodyne frequencies with high associated data rates to be obtained. The combination of ac confocal phase microscopy and new detector technology will pave the way for new applications, which are extremely difficult to develop with current phase-stepping techniques. Another advantage is that a fully heterodyne system can be rendered extremely stable by use of an optically generated local oscillator and lock-in detection.

The authors acknowledge support from the Engineering and Physical Sciences Research Council, UK, for this work. M. C. Pitter's e-mail address is mark.pitter@nottingham.ac.uk.

## References

1. T. Tkaczyk and R. Józwicki, *Opt. Eng.* **42**, 2391 (2003).
2. N. A. Massie, M. Dunn, D. Swain, S. Muentner, and J. Morris, *Appl. Opt.* **22**, 2141 (1983).
3. M. G. Somekh, C. W. See, and J. Goh, *Opt. Commun.* **174**, 75 (2000).
4. S. Bourquin, V. Monterosso, P. Seitz, and R. P. Salathé, *Opt. Lett.* **25**, 102 (2000).
5. S. Ando and A. Kimachi, *IEEE Trans. Electron. Devices* **50**, 2059 (2003).
6. M. C. Pitter, J. Y. L. Goh, M. G. Somekh, B. R. Hayes-Gill, M. Clark, and S. P. Morgan, *Electron. Lett.* **39**, 1339 (2003).
7. A. L. Migdall, B. Roop, Y. C. Zheng, J. E. Hardis, and G. J. Xia, *Appl. Opt.* **29**, 5136 (1990).
8. A. Dubois, L. Vabre, A.-C. Boccara, and E. Beaufrepaire, *Appl. Opt.* **41**, 805 (2002).
9. P. Carre, *Metrologia* **2**, 13 (1966).